The Expulsion of Magnetic Flux by Eddies

N. O. Weiss

References	**Article cited in:** http://rspa.royalsocietypublishing.org/content/293/1434/310#related-urls
Email alerting service	Receive free email alerts when new articles cite this article - sign up in the box at the top right-hand corner of the article or click **here**

The expulsion of magnetic flux by eddies

By N. O. Weiss

U.K.A.E.A., Culham Laboratory, Abingdon, Berkshire

A convective eddy imposed on an initially uniform magnetic field in a highly conducting
fluid distorts the lines of force and amplifies the field. Flux is concentrated outside the eddy;
within it, the field grows and its scale of variation decreases until resistive effects become
important. Closed lines of force are then formed by reconnexion. The central field decays
and a steady state is reached. Within a period, small compared with the characteristic time
for resistive decay, magnetic flux is almost entirely expelled from regions of rapid motion and
concentrated at the edges of convection cells. This process is demonstrated from numerical
experiments. The results are applied to the sun, where the concentrated fields are strong
enough to inhibit convection locally.

1. Introduction

Magnetic fields are associated with convection in the chromosphere, the photosphere
and the hydrogen convection zone of the sun; they are involved in the turbulent
motions of interstellar gas and, on a less grand scale, similar effects are produced by
instabilities in laboratory plasmas. In all these circumstances, the medium is highly
conducting (the magnetic Reynolds number may vary from 10^3 in an experiment to
10^{17} in the galaxy) and so the motions distort and amplify the field. Reconnexion of
the lines of force then changes its configuration. In order to explain this process it
is necessary to attain some quantitative understanding of the interaction (Weiss
1964*b*).

It is therefore worth considering a more straightforward problem in detail.
The simplest relevant model is an isolated eddy (corresponding to a convection cell)
imposed on an initially uniform magnetic field in a magnetohydrodynamic fluid of
small but finite resistivity. The magnetic field is dragged round by the motion and
the field energy consequently rises. In time, the lines of force relink—with the
formation of X and O-type neutral points—and a new configuration is established:
magnetic flux is almost entirely excluded from regions where rapid motions prevail
and is concentrated at the edges of the cell (Weiss 1964*a*).

The actual time-dependent behaviour is followed in detail in this paper, which
demonstrates the formation of closed lines of force by reconnexion. The process is
completed in a time smaller than the characteristic resistive decay time for the
system. Amplified magnetic fields are created, whose magnitude can be estimated in
terms of the magnetic Reynolds number.

This model assumes an inexorable motion in an incompressible fluid. Turbulent
convection is less regular and more complicated. Moreover, the enhanced magnetic
fields are strong enough to affect the motion which produces them. Nevertheless,
it is possible to estimate the effects of convection on magnetic fields in the sun.
In particular, it seems likely that in the deep convective zone magnetic flux is

[310]

concentrated into ropes (Weiss 1964 a, b). Simon & Leighton (1964) have observed a similar concentration at the edges of chromospheric supergranules.

The problem of calculating the induced field in a conducting sphere rotating rapidly within an insulator is fairly venerable (Thomson 1893). The related case of a sphere or cylinder enclosed by a conductor has been discussed by Bullard (1949) and others (Herzenberg & Lowes 1957; Moffatt 1965). Sweet (1950) and Herzenberg & Lowes (1957) considered the amplification of a magnetic field by an isolated eddy. Lines of force that run across the motion are rapidly sheared and their dissipation is enhanced; on the other hand, field components parallel to the streamlines are unaffected by the motion (Sweet 1949; Cowling & Hare 1957). E. N. Parker (1963 b) has found analytical solutions for steady magnetic fields in the presence of certain fluid flows, showing that the lines of force are concentrated into restricted regions where the magnetic field and velocity vectors are nearly parallel. More recently, R. L. Parker (1966) has obtained, analytically, the time-dependent solution for a rotating sphere or cylinder.

2. The model problem

All results in this paper are based on numerical computations carried out on the I.B.M. 7030 (Stretch) computer at A.W.R.E., Aldermaston. These calculations cover several related problems: an isolated eddy in an initially uniform field, a band of eddies (simulating a convective layer) in both horizontal and vertical fields and a double band of eddies (to indicate the effects of a small scale-height). The treatment is purely kinematic; that is to say, the velocity $\mathbf{u}$ does not vary with time, dynamics are ignored and there is no reaction of the magnetic field $\mathbf{B}$ back upon the motion. Thus the results are only valid if the magnetic energy remains insignificant compared with the kinetic energy of the motion, i.e. if

$$B^2/8\pi\mu \ll \tfrac{1}{2}\rho u^2. \tag{1}$$

For simplicity, the calculation is restricted to two-dimensional incompressible flow. The streamlines are closed and

$$\operatorname{div}\mathbf{u} = 0. \tag{2}$$

For a medium with a constant conductivity σ, Maxwell's equations reduce to

$$\partial\mathbf{B}/\partial t = \operatorname{curl}(\mathbf{u}\wedge\mathbf{B}) + \eta\nabla^2\mathbf{B} \tag{3}$$

and div $\mathbf{B} = 0$, where the resistivity $\eta = (4\pi\mu\sigma)^{-1}$. Let both $\mathbf{B}$ and $\mathbf{u}$ be confined to the xy plane. Then $\mathbf{B}$ can be described by a stream function (the z component of the vector potential) A such that

$$\mathbf{B} = \left(\frac{\partial A}{\partial y}, -\frac{\partial A}{\partial x}, 0\right). \tag{4}$$

Equation (3) then simplifies to

$$\partial A/\partial t = -\mathbf{u}.\nabla A + \eta\nabla^2 A \tag{5}$$

or, from (2), to

$$\partial A/\partial t = -\operatorname{div}(A\mathbf{u} + \eta\nabla A). \tag{6}$$

This is the conservation equation for a scalar, such as mass, with a small diffusion term included.

In a system with a characteristic dimension L and a characteristic speed U, the ratio of the first (convective) to the second (diffusive) term on the right hand side of (3) or (5) is given by the magnetic Reynolds number,

$$R_m = UL/\eta. \tag{7}$$

This parameter determines the behaviour of the field: when R_m is large (small resistivity) diffusion is dominated by convection.

The numerical methods required to solve (6) are discussed elsewhere (Roberts & Weiss 1966). In order to achieve sufficient accuracy with a reasonable number of mesh points it is necessary to adopt a finite difference scheme with fourth order accuracy. This involves using a mesh on which alternate points are staggered in time; calculating a new value of A at one grid point then requires values at eight neighbouring points. It is convenient to impose rigorous boundary conditions at the edges of a rectangular region (rather than at infinity as one would in attempting an analytical solution). The upper and lower boundaries are therefore assumed to be perfectly conducting, so that lines of force are tied to them, while the system is assumed to be periodic in the horizontal direction. Special treatment is required for points on the boundary, or at a discontinuity in velocity (which may be regarded as an internal boundary).

The machine time required to solve a problem varies inversely as the cube of the mesh interval. The calculations were done using a grid of 50×50 points (and some were confirmed by runs on a 100×100 mesh) on which values of R_m in the range 20 to 1000 could be accurately treated. Each such run generates about 10^6 numbers and some form of graphical ouput is necessary for presenting the results. Fortunately, it is easy to plot the lines of force, which are just contours of constant A. These are produced on microfilm after each timestep of the calculation, with the aid of a Stromberg–Carlsen 4020 recorder; the 35 mm film can then be converted to 16 mm and run as a movie. This is indeed the proper way to present such results, for the reconnexion of lines of force, the production and the decay of closed loops can all be followed visually as they occur.

In the absence of a film, the behaviour of the magnetic field is better described by drawing lines of force than it is by any commentary. The following section presents a series of such diagrams, accompanied by brief descriptions.

3. Numerical results

The induction equation (6) is integrated over the square region $|x| \leqslant \frac{1}{2}L, |y| \leqslant \frac{1}{2}L$, within which $\mathbf{u}$ has a maximum magnitude U. It is convenient to choose units of length and time so as to make both L and U equal to unity. Then the magnetic Reynolds number is just the reciprocal of the resistivity:

$$R_m = 1/\eta.$$

Interpretation of R_m thus depends on the velocity pattern, since L is defined by the size of the region rather than the scale of the motion. There are two characteristic times associated with this region, the turnover time for the eddy (an estimate of the time taken to carry material from the bottom to the top)

$$\tau_0 = L/U \tag{8}$$

and the characteristic time for resistive decay

$$\tau_\eta = L^2/4\pi^2\eta. \tag{9}$$

The choice of units means that time is measured in terms of τ_0. Just as $\mathbf{B}$ is defined by A in (4), so the solenoidal velocity $\mathbf{u}$ is defined in terms of a stream function Ψ which has to be chosen appropriately for each problem.

(a) *Isolated eddy*

Characteristic phenomena are clearly displayed with a single isolated eddy, bounded by a discontinuity in velocity, whose stream function is given by

$$\Psi = -(1/2\pi)\cos 2\pi x \cos 2\pi y \quad (|x| \leqslant \tfrac{1}{4}, |y| \leqslant \tfrac{1}{4}),$$
$$= 0 \quad (|x|, |y| > \tfrac{1}{4}).$$

Velocity streamlines and lines of force of the initial field are shown in figure 1 (a) and (b) respectively.

If the magnetic Reynolds number is low, the field is distorted by the motion, but a steady state is soon reached in which matter streams past the lines of force and convection is balanced by diffusion. When $R_m = 20$, the field settles down by the time $t = 1 \cdot 0$; with $R_m = 50$, the final state is not reached till $t = 1 \cdot 5$. These steady configurations are shown in figure 1 (c) and (d); the central field is slightly diminished but no reconnexion takes place.

With $R_m = 1000$, the behaviour of the magnetic field is quite different, as appears in figure 1 (e) to (j). The lines of force are abruptly sheared and a strong field is built up at the edge of the eddy. Reconnexion takes place, the closed field lines decay and disappear; by $t = 4 \cdot 0$ a steady state has been achieved in which almost all the flux has been ejected from the eddy and concentrated outside it. (The characteristic time for resistive decay, $\tau_\eta = 6 \cdot 25$.)

(b) *Single eddy*

An eddy in which the velocity drops continuously to zero at the boundaries forms a better model of a convection cell. Because of the boundary conditions at $y = \pm \tfrac{1}{2}$ it is necessary to choose a pattern of motion that falls off rapidly at top and bottom. The streamlines corresponding to

$$\Psi = -(1/\pi)(1 - 4y^2)^4 \cos \pi x \tag{10}$$

are shown in figure 2 (a).

The final configuration with $R_m = 40$ is displayed in figure 2 (b) and successive stages in the distortion of the field for $R_m = 1000$ appear in figures 2 (c) to (j). A strong field is built up near $x = \pm \tfrac{1}{2}$ and the lines of force relink where there is the greatest shear in $\mathbf{u}$. This process is completed by $t = 4 \cdot 0$; the resistive decay time $\tau_\eta \sim 25$. The final configuration of figure 2 (d) may be compared with figure 6, obtained with $R_m = 200$.

(c) *Band of eddies*

A convection layer concentrates a vertical field into the regions between the eddies. The stream function

$$\Psi = -(1/4\pi)(1 - 4y^2)^4 \sin 4\pi x \tag{11}$$

gives a band of eddies rotating in alternate senses, whose streamlines are depicted in figure 3(a). Figure 3(b) shows that magnetic flux is concentrated into ropes between the cells.
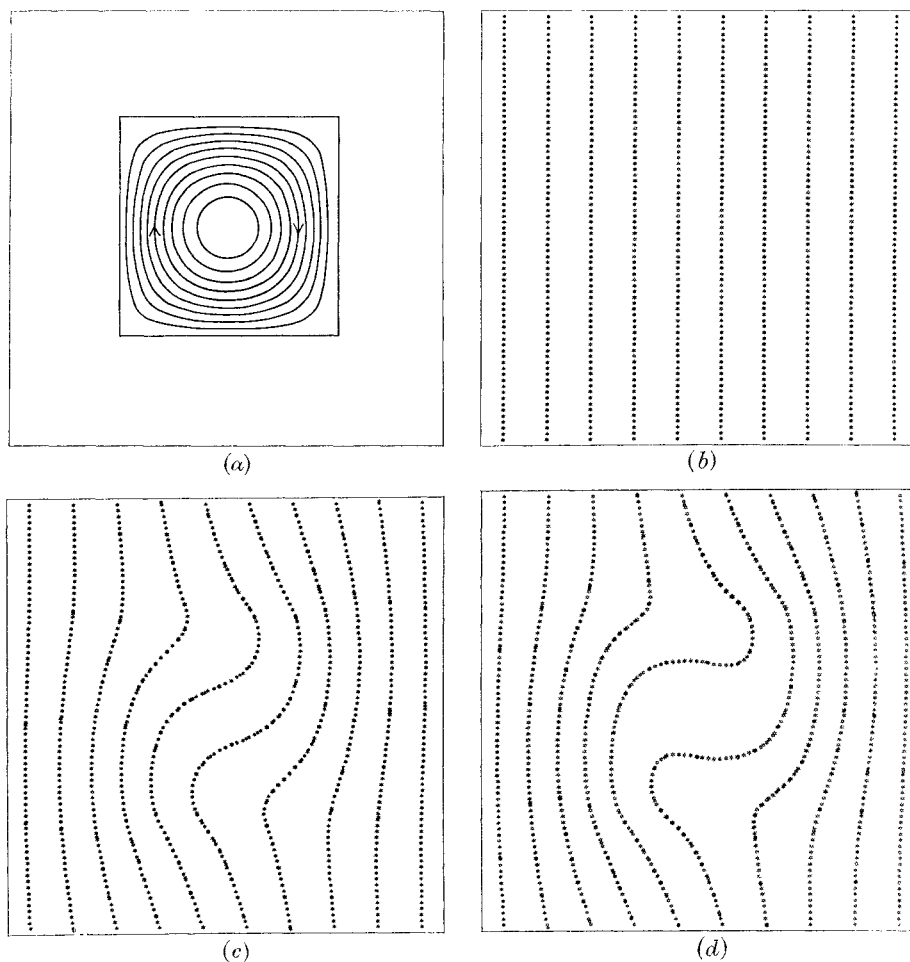

FIGURE 1 (for legend see next page)

(d) *Double band of eddies*

The depth of the solar convection zone is greater than the scale of convective eddies. That the flux will be concentrated into regions of rising and falling material is indicated in figure 3(d), which shows the final configuration achieved with $R_m = 1000$. The velocity is that of figure 3(c), defined by a stream function

$$\Psi = (1/4\pi)\sin 2\pi x \sin 4\pi y \quad (|y| \leqslant \tfrac{1}{4})$$
$$= 0 \quad (|y| > \tfrac{1}{4}).$$

(e) *Band of eddies in a horizontal field*

An initially horizontal field is expelled from a convecting layer and concentrated at its limits. This is illustrated in figure 4 for the pattern of eddies defined by (11). When $R_m = 1000$ the steady state is reached by $t = 3 \cdot 0$.
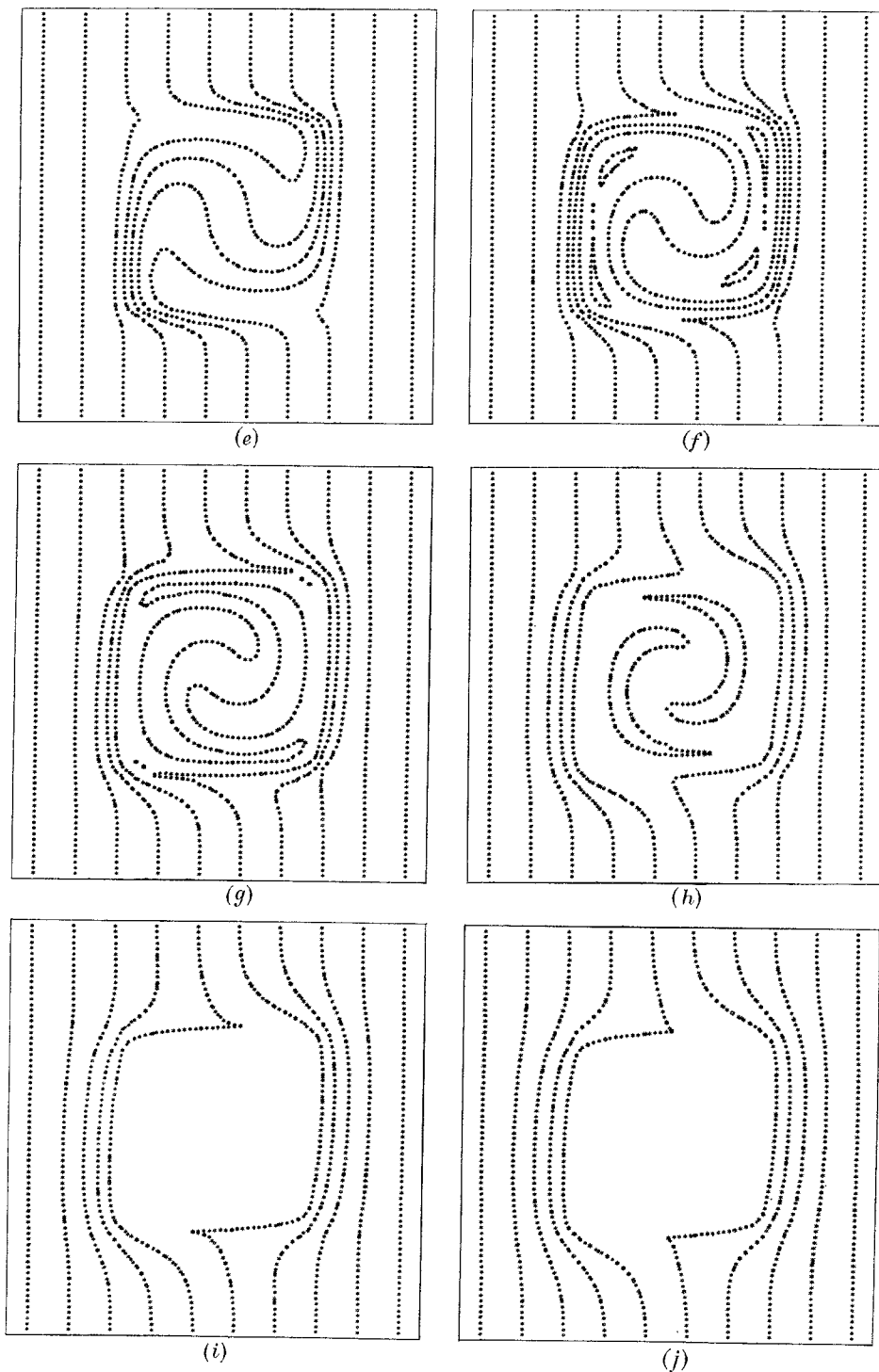
FIGURE 1. Expulsion of flux from an isolated eddy. At low R_m the field is distorted without reconnexion taking place; at high R_m the field is first amplified, then lines of force reconnect and finally flux is expelled from the eddy and a steady state is reached. (a) Velocity streamlines. (b) Initial magnetic field. (c) and (d) Final states for $R_m = 20$ and 40 respectively. Sequence with $R_m = 1000$: (e) $t = 0\cdot5$, (f) $t = 1\cdot0$, (g) $t = 1\cdot5$, (h) $t = 2\cdot0$, (i) $t = 3\cdot0$, (j) $t = 4\cdot0$.
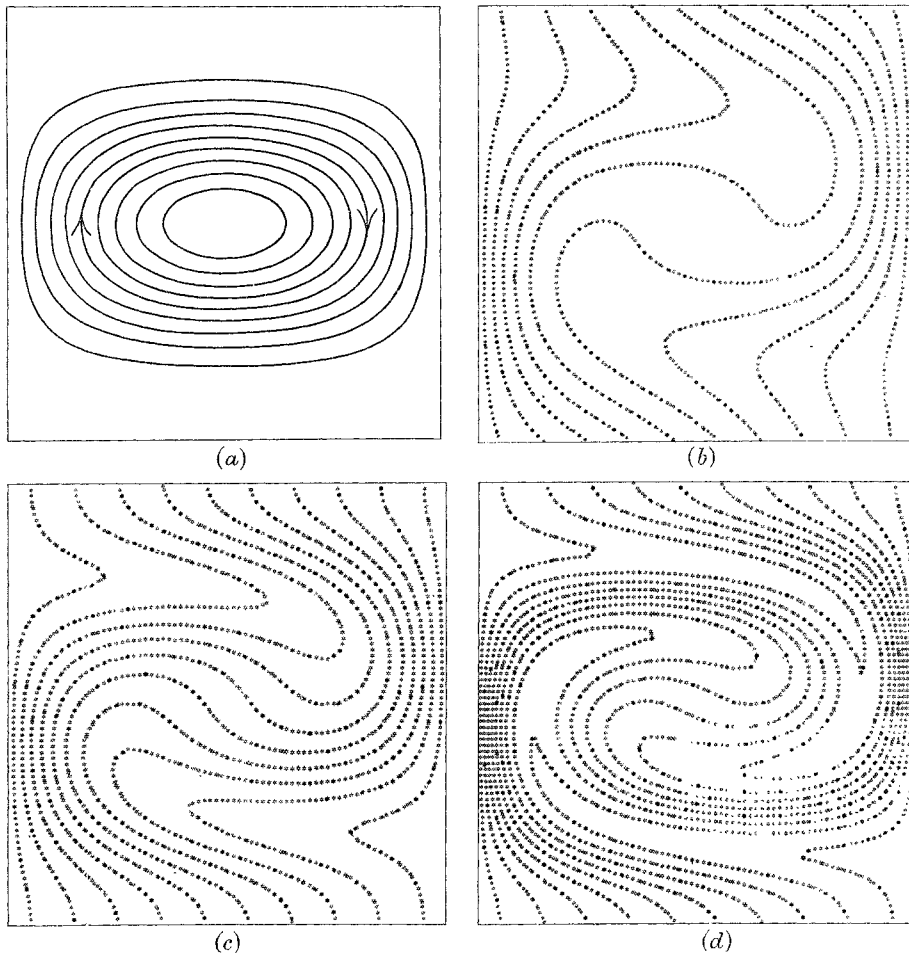
N. O. Weiss

FIGURE 2 (for legend see next page)

4. PHYSICAL INTERPRETATION

The behaviour of the field is clear from figures 1 to 4: the flux is initially concentrated at the edges of the cell and amplified within the eddy; subsequently the lines of force reconnect, the central field decays and the configuration relaxes to a steady state. It is convenient to follow this process by plotting the average magnetic energy density, $\langle B^2 \rangle$, as a function of time. Curves for the single eddy defined by (10) are shown in figure 5. The numerical results are confined to two-dimensional problems; three-dimensional motions will be mentioned later.

Initially there is a uniform field with magnetic energy B_0^2. Any distortion must increase $\langle B^2 \rangle$. For small values of the magnetic Reynolds number, $\langle B^2 \rangle$ rises only slightly and rapidly settles to a steady value (see curves a and b of figure 5). For large R_m, the energy increases to a maximum value B_1^2; then reconnexion occurs and $\langle B^2 \rangle$ falls to a steady value of B_2^2: the flux is expelled from the eddy and concentrated into restricted regions with a strong field B_3. Then

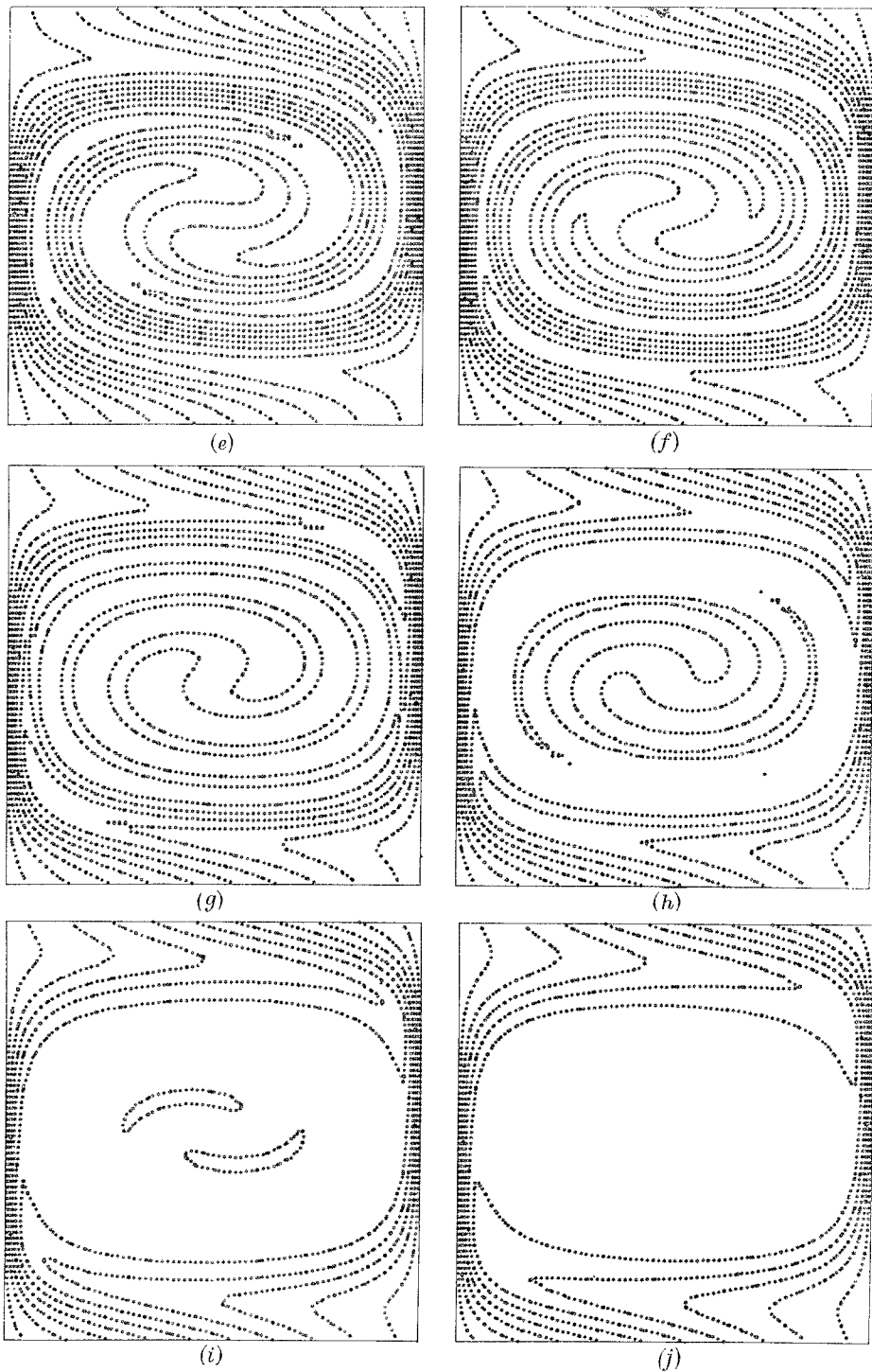$$B_0^2 < B_2^2 < B_1^2 < B_3^2. \tag{12}$$

FIGURE 2. Expulsion of flux from a single eddy. Flux is rapidly concentrated at the edges of the cell. The central field is amplified and finally decays. (a) Velocity streamlines. (b) Final state with $R_m = 40$. Sequence with $R_m = 1000$: (c) $t = 0.5$, (d) $t = 1.0$, (e) $t = 1.5$, (f) $t = 2.0$, (g) $t = 2.5$, (h) $t = 3.0$, (i) $t = 3.5$, (j) $t = 4.0$.

Simple physical arguments provide estimates of these fields in terms of the magnetic Reynolds number.

The convective and resistive terms in the induction equation (3) may be considered separately. The eddy builds up the component $B_{\parallel}$ of $\mathbf{B}$ parallel to the motion by the interaction of $\mathbf{u}$ and the perpendicular component $B_{\perp}$. Therefore the convective term is of order uB_0/L and does *not* increase with time. Thus $B_{\parallel} \propto t$.
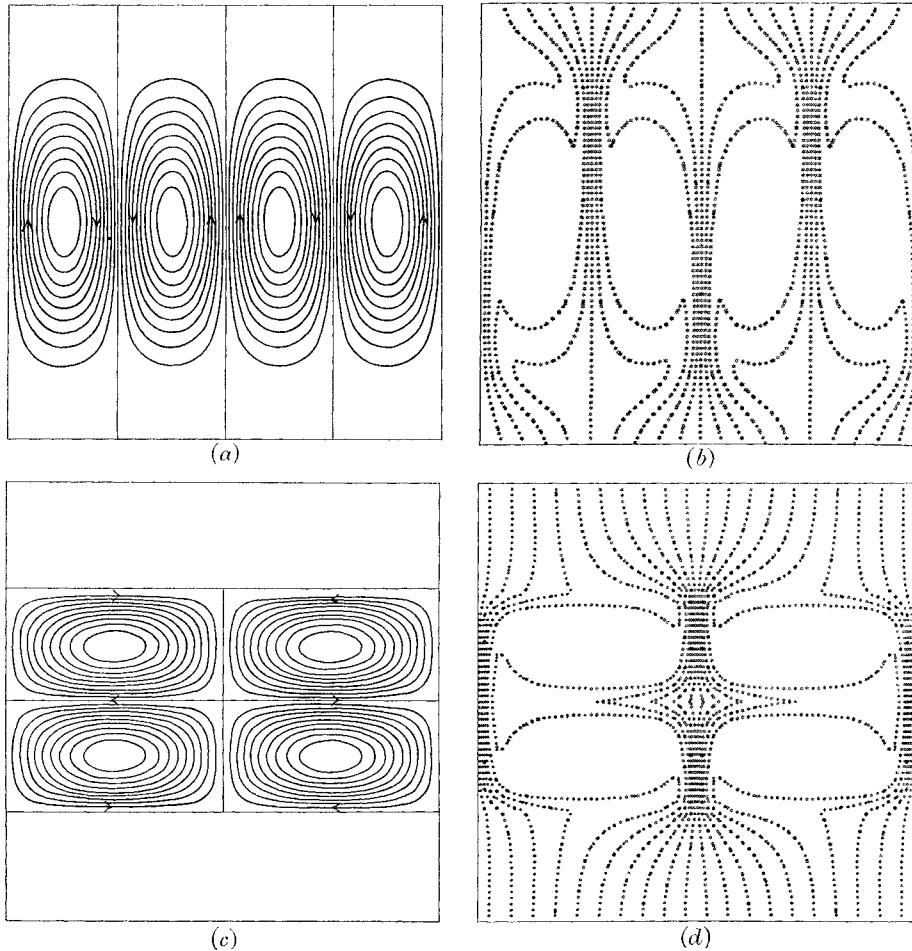

FIGURE 3. Concentration of flux into ropes by a convective layer ($R_m = 1000$). Single band of eddies: (a) velocity streamlines, (b) steady field. Double band of eddies: (c) velocity streamlines and (d) steady field.

Simultaneously, the scale of variation for $B_{\parallel}$ decreases. For a simple eddy, this scale changes after a time t from L to

$$l \sim \frac{B_0}{B} L \sim \frac{L^2}{Ut} = \frac{\tau_0}{t} L.$$

The resistive term, on the other hand, is of order

$$\frac{\eta B}{l^2} \sim \frac{\eta}{L^2} \left(\frac{B}{B_0}\right)^3 B_0. \tag{13}$$
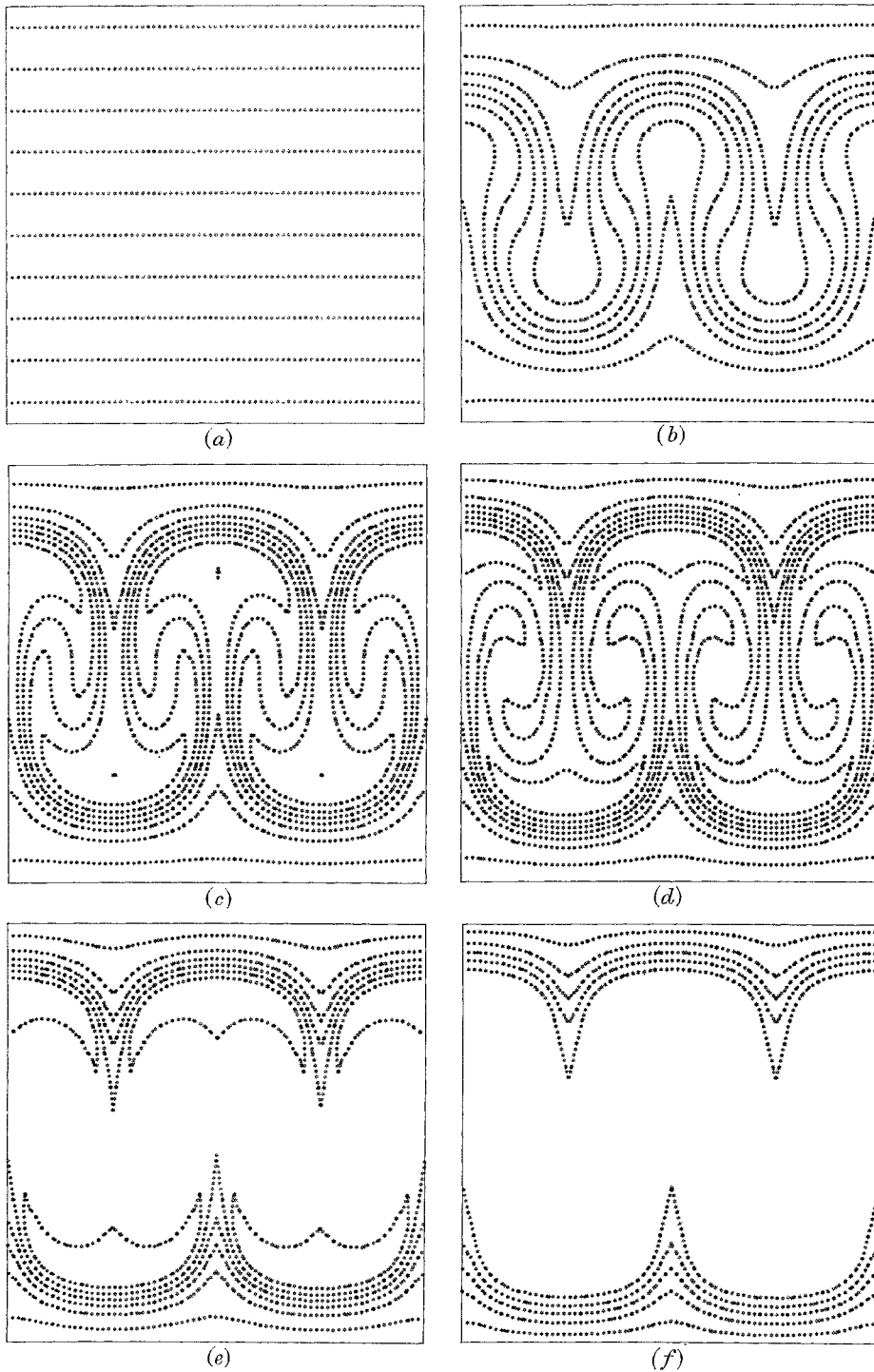
FIGURE 4. Expulsion of a horizontal field from a convective layer. Sequence with $R_m = 1000$: (a) $t = 0 \cdot 0$, (b) $t = 0 \cdot 5$, (c) $t = 1 \cdot 0$, (d) $t = 1 \cdot 5$, (e) $t = 2 \cdot 0$, (f) $t = 3 \cdot 0$.

320 N. O. Weiss

Amplification of the field continues until resistive effects are comparable with convection. Reconnexion then becomes important. This occurs when

$$|\mathrm{curl}\,(\mathbf{u} \wedge \mathbf{B})| \sim |\eta \nabla^2 \mathbf{B}|. \tag{14}$$

Then

$$\frac{UB_0}{L} \sim \frac{\eta B}{l^2}$$

or, from (7) and (13),

$$B \sim R_m^{\frac{1}{3}} B_0.$$

Thus the maximum value of $\langle B^2 \rangle$,
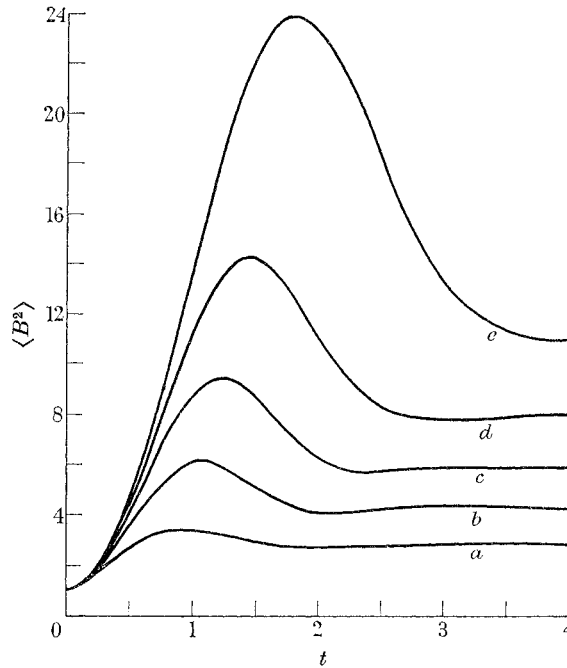
$$B_1^2 \sim R_m^{\frac{2}{3}} B_0^2. \tag{15}$$

FIGURE 5. Magnetic energy as a function of time. Curves labelled a, b, c, d, e have $R_m = 40, 100, 200, 400, 1000$ respectively.

The central field then diminishes through diffusion until $\langle B^2 \rangle$ settles to a steady value. (The curves of figure 5 indicate that $\langle B^2 \rangle$ falls and then rises slightly as the field adjusts itself to the new configuration; this is a physical and not a numerical effect.) Two further points need emphasis. First, it is clear from symmetry that one line of force must always pass through the centre, so not all the flux is eliminated from the eddy. Secondly, the central field may continue to fluctuate long after $\langle B^2 \rangle$ has reached its final value. In figure 6 the line of force through the centre is plotted for $R_m = 200$, first when $t = 2 \cdot 5$ (and $\langle B^2 \rangle$ has just reached a steady value) and then for $t = 6 \cdot 0$. During this interval, the central field is still changing and this line continues to reconnect itself; after $t = 6 \cdot 0$ the configuration remains fixed. Meanwhile, the field at the centre has fallen from 30 to 5 % of its initial value. Yet the total effect of this residual field is negligible, for $\langle B^2 \rangle$ does not vary perceptibly after $t = 2 \cdot 5$ (see curve c of figure 5).

Of course, the time required for $\langle B^2 \rangle$ to achieve its maximum and then to settle down, as well as the time taken for the field to reach a steady state, depend on the nature of the shear in **u**. The physical arguments adduced above really apply to a simple model in which the angular velocity falls off linearly with radius. This does not hold near the origin for the velocity defined by (10), hence the time taken to reach the final steady field. In the model treated by R. L. Parker, the velocity shear is restricted to a discontinuity. Then the outer field is almost immediately disconnected, in a time of order τ_0, while diffusion can only affect the central field after a period τ_η. Thus the time scales in Parker's problem cannot be related to those discussed here.
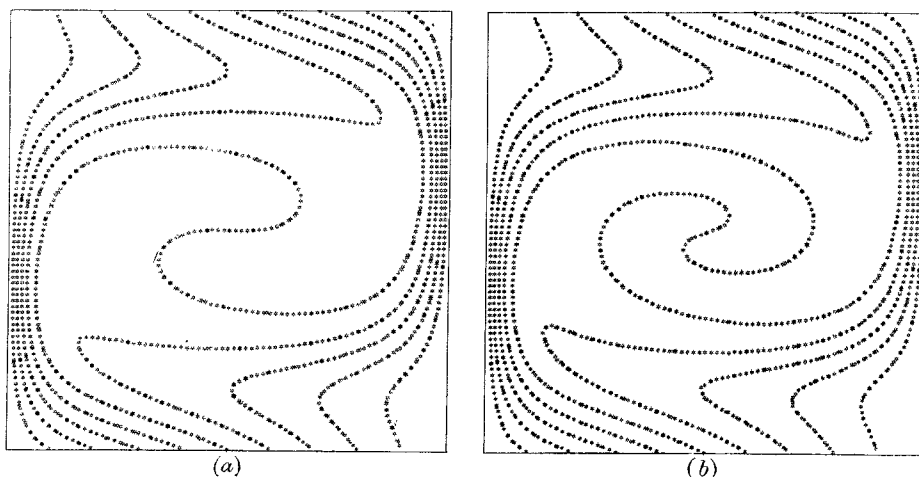

FIGURE 6. Changing field at the centre of the eddy. Single eddy as in figure 2 but with $R_m = 200$ and the central line of force plotted: (a) $t = 2\cdot5$ and (b) $t = 6\cdot0$.

The field is rapidly swept aside to the edges of the eddy, where flux is concentrated into regions of width d centred on rising or falling currents. Within these magnetic boundary layers, convection is balanced by diffusion. The transverse velocity u_x increases linearly with x:

$$u_x = -\pi x U/L \quad (x \ll L). \tag{16}$$

Then, from (14)
$$d \sim R_m^{-\frac{1}{2}} L,$$

as has been pointed out by Clark (1965), whence

$$B_3^2 \sim R_m B_0^2. \tag{17}$$

In fact, a field with a y component only in the presence of the velocity (16) has a steady state with a Gaussian profile:

$$B_y = (2R_m)^{\frac{1}{2}} B_0 \exp\left(-\pi R_m x^2/2L^2\right). \tag{18}$$

Almost all the magnetic energy is concentrated into the region with $x \lesssim d$. Thus the final value of $\langle B^2 \rangle$ can be estimated as

$$B_2^2 \sim R_m^{\frac{1}{2}} B_0^2. \tag{19}$$

The curves in figure 5 show runs made with five different values of R_m in the range 40 to 1000. The corresponding values of B_1^2, B_2^2 and B_3^2 are plotted logarithmically against R_m in figure 7. The points lie on the lines labelled a, b, c with slopes 0·59, 0·42, 1·00 respectively. These values agree well enough with the predictions of (15), (19) and (17).
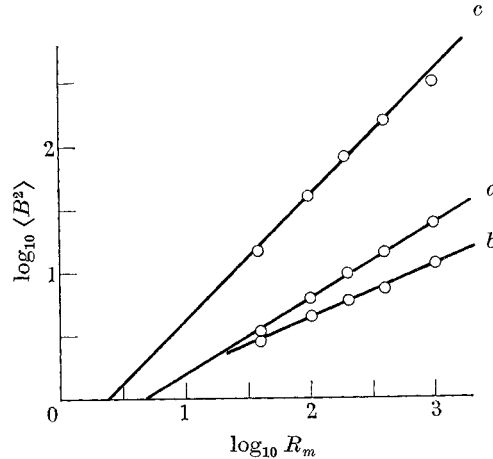

FIGURE 7. Magnetic energy as a function of R_m. The lines labelled a, b, c refer to B_1^2, B_2^2 and B_3^2 respectively.

Finally, these results are consistent with the assumption that the time τ taken for $\langle B^2 \rangle$ to reach a steady value is given by

$$\tau \sim R_m^{\frac{1}{3}} \tau_0. \tag{20}$$

For large magnetic Reynolds numbers this is much less than the resistive decay time

$$\tau_\eta \sim R_m \tau_0 \sim R_m^{\frac{2}{3}} \tau.$$

Thus flux is expelled from the eddy in a time short compared with the time scale for resistive decay over a region of dimension L.

In three dimensions, simple convection cells can be constructed from two-dimensional motions confined to vertical, distorted sheets; reconnexion then proceeds as described above. For less special motions, the amplified field varies inversely as the square of the characteristic distance l. Consequently

$$B_1 \sim R_m^{\frac{1}{2}} B_0 \tag{21}$$

instead of being proportional to $R_m^{\frac{1}{3}}$. The superficially identical argument employed by E. N. Parker (1963a) applies to turbulent rather than to persistent motions and yields an r.m.s. field

$$B \sim R_m^{\frac{1}{4}} B_0.$$

At the vertices of the cell the flux is rapidly concentrated into a column whose radius is proportional to $R_m^{-\frac{1}{2}}$. Thus the field now varies as R_m rather than $R_m^{\frac{1}{2}}$ and the energy density,

$$B_3^2 \sim R_m^2 B_0^2. \qquad\qquad \text{and}$$

More precisely, the horizontal velocity near the vertices of a square cell of side L has the form
$$\mathbf{u}_\perp = -(2\pi U/L)\mathbf{r},$$
which, for $R_m \gg 1$, gives rise to a steady vertical field:
$$B = R_m B_0 \exp(-\pi R_m r^2/L^2).$$

5. Turbulent convection

In the last three sections the precise behaviour of a simple model has been analysed. Convection is generally far more complicated: to what extent can the conclusions reached above be applied to real problems? The insight gained helps in predicting the nature of turbulent magnetic fields whose detailed behaviour is difficult to describe.

The turbulent velocity is a function of time and the pattern of motions loses its identity after a period of order τ_0. An eddy does not persist for long enough to eliminate the field from its centre. On the other hand, the presence of eddies on a smaller scale accelerates the annihilation of sheared magnetic fields. Moreover, resistive instabilities may facilitate the development of such eddies.

Nevertheless, magnetic flux will still be swept into restricted regions, with strong fields. This process is very rapid, though not instantaneous. Consider, for the moment, an eddy in a perfectly conducting fluid: after it has turned over once, the concentrated field will have risen from B_0 to B_t, say. The value of B_t depends on the nature of the motion. However, for a typical three-dimensional eddy
$$B_t \sim (10^3 \text{ to } 10^4)\, B_0 \tag{23}$$
(see Appendix). Thus $B_t > B_3$ and the concentration of the field to its final value is effectively immediate for all $R_m \lesssim 10^3$.

The foregoing discussion has assumed that
$$B^2 \ll 4\pi\rho u^2$$
everywhere, throughout the process. There is certainly no reason to suppose that equipartition must be established for every initial field B_0.† However, the amplified fields B_1 and B_3 frequently violate this condition. Clearly, convection cannot compress magnetic flux after the magnetic and kinetic energy densities become comparable. Thus there is an upper limit B_e to the fields that can be produced by eddies, i.e.
$$B^2 \leqslant B_e^2 \sim 4\pi\rho U^2. \tag{24}$$

Once this limit is reached, the electromagnetic forces will react upon the motions and the velocity pattern may change in consequence. For example, three-dimensional convection would tend to concentrate the field round the perimeter of a cell ($B_3 \propto R_m^{\frac{1}{2}}$) rather than at the corners ($B_3 \propto R_m$).

To sum up, it seems probable that turbulent convection concentrates the field into restricted regions, or ropes of flux, until it is checked either by finite resistivity or by the finite lifetime of the eddy, or until fields are strong enough to prevent any motion across themselves. Whichever of the fields B_3, B_t and B_e defined by (22),

---

† Nor will $\mathbf{B}$ necessarily behave like the vorticity $\boldsymbol{\omega}$: for magnetic flux is liable to be concentrated into just those regions where $|\boldsymbol{\omega}|$ is least.

(23) and (24) is least thus imposes an upper limit on the field that is produced. Magnetic fields will not be utterly eliminated from intervening regions but it seems likely that the large scale field is concentrated into ropes. Once established, these strong fields may change position as the convection pattern alters but they will remain at the boundaries of convection cells.

6. APPLICATIONS

(a) Laboratory experiments

Unfortunately, these predictions are not easy to test experimentally. In some toroidal z pinches, instabilities arise with motion in rolls about the helical field lines. These only occur at values of the radius for which the rotational transform is a multiple of 2π. Ware (private communication) has explained the measured variation of the transverse field (Ware, Forsen & Schupp 1962) on the hypothesis that it is expelled from the rolls and concentrated in between them.

An analogous situation arises with a rotating magnetic field. Under certain conditions the ions remain fixed while the electrons are tied to the field lines. The behaviour of the field is similar to the model discussed in §3 (a) and the weakened field has been detected experimentally (Blevin & Thonemann 1962; Thonemann & Kolb 1964, Kolb, Thonemann & Hintz 1965).

(b) Solar magnetic fields

Turbulent convection in the sun gives magnetic Reynolds numbers of order 10^6 to 10^{10}. This requires considerable extrapolation from the results of numerical experiments with $R_m \leqslant 1000$. Moreover, the concentrated fields are frequently strong enough to interfere with the convective motions. Thus it is necessary to solve the full dynamical problem, for which the kinematic treatment is only a preliminary stage. But it is now possible to answer two questions: first, by what factor will the field be amplified? Secondly, given the average flux density in the region concerned, will the equipartition field B_e be reached and therefore set a limit to the amplification process? If so, it is likely that magnetic flux will be concentrated into sheets or ropes with fields strong enough to inhibit convection. The dynamical behaviour of these flux ropes requires further investigation.

Convective zone

In the deep convective zone the magnetic Reynolds number is around 6×10^{10}. If the flux through the convective zone were uniformly distributed, there would be a field of about 1 G. The extent to which this would be amplified is shown in table 1. (The two values for B_3 depend on whether the field is concentrated in the corners or merely along the edges of convection cells). From the table,

$$B_e \sim B_l \ll B_3.$$

Ropes of flux are therefore likely to be formed, with fields of about 5000 G. The occurrence of discrete magnetic regions in the photosphere supports this hypothesis (Weiss 1964b).

Chromosphere

It has been demonstrated (Simon & Leighton 1964; Leighton 1959; Leighton, Noyes & Simon 1961; Leighton 1963) that magnetic fields are concentrated at the boundaries of supergranules and that the field structure is related to the chromospheric network. The origin of these large-scale motions is uncertain; however, table 1 shows that $B_3 \gg B_e$ and the field should therefore be concentrated until it interferes with the convection. The observed fields of order 10 to 100 G agree with this prediction.

TABLE 1. MAGNETIC FIELDS (IN GAUSS) IN THE SUN

	convective zone	chromospheric supergranules	photosphere	
			undisturbed	active
R_m	6×10^{10}	10^7	10^6	
B_0	1	1	0·1	10
$B_1 \ (R_m^{\frac{1}{3}} B_0)$	4×10^3	2×10^2	10	10^3
$B_3 \ (R_m \ B_0)$	6×10^{10}	10^7	10^5	10^7
$\quad (R_m^{\frac{1}{2}} B_0)$	2×10^5	3×10^3	10^2	10^4
$B_e \ (4\pi\rho U^2)^{\frac{1}{2}}$	5×10^3	10	6×10^2	

Photosphere

Eddy motions in granules should amplify any fields that may be present in undisturbed regions of the sun but not enough to affect convection. On the other hand, the concentration of magnetic fields in active regions ought to have detectable effects. Yet no change in the lifetime or structure of the granules has been observed. At the levels where fields can be measured the velocity must be confined to vertical oscillatory motions (Leighton 1963), for concentrated fields have not been found.

Sunspots

Danielson (1961) has convincingly explained penumbral filaments but the apparent cellular structure of the umbra (Danielson 1964; Bray & Loughhead 1964) is difficult to understand. Recent estimates of the umbral conductivity suggest a value of only 10^{10} e.s.u. The magnetic Reynolds number in umbral granules may thus be as low as 20, in which case matter could stream past lines of force without producing much distortion.

APPENDIX. TURNOVER TIMES AND CONCENTRATION OF FLUX

The process of concentration is rapidly accomplished; when $R_m = 1000$ the field between eddies achieves its final value almost immediately (see figure 3). Nevertheless, the time required does become significant when $R_m > 10^4$, as was mentioned in §5. This time scale has been studied for a simple upwelling (Parker 1963b; Clark 1965). In a typical convection cell it is necessary to calculate the turnover time before the lifetime of the eddy and the rate of concentration of flux can be estimated.

(a) Turnover times for two- and three-dimensional eddies

Consider first the two-dimensional eddy defined by the stream function

$$\psi = -\cos x \cos z \quad (|z| \leqslant \tfrac{1}{2}\pi), \tag{25}$$

whose streamlines are given by the family of curves

$$\cos x \cos z = \cos \xi = k \quad (1 \geqslant \cos^2 x \geqslant \cos^2 \xi).$$

Then the parameter ξ labels the streamline passing through the points $(0, \pm \xi)$ and $(\pm \xi, 0)$. The turnover time, τ, is a function of ξ. It is convenient to calculate the quarter period,

$$t(\xi) = \tfrac{1}{2}\tau(\xi) = \int_0^\xi \frac{\mathrm{d}x}{u_x} = \int_0^\xi \frac{\mathrm{d}x}{(\cos^2 x - k^2)^{\frac{1}{2}}},$$

and to make the substitution

$$\sin x = \sin \xi \sin w.$$

Then

$$t(\xi) = \int_0^{\frac{1}{2}\pi} \frac{\mathrm{d}w}{(1 - \sin^2 \xi \sin^2 w)^{\frac{1}{2}}},$$

the complete elliptic integral of the first kind. If

$$\delta = \tfrac{1}{2}\pi - \xi \ll \tfrac{1}{2}\pi,$$

then

$$t(\xi) \doteqdot \ln(4/\sin \delta) \quad \text{and} \quad \delta \doteqdot 4\,\mathrm{e}^{-t}.$$

The central region rotates as a solid body and $t(0) = \tfrac{1}{2}\pi$ but the turnover time becomes infinite at the edge of the eddy. The ratio $t(\xi)/t(0)$ is tabulated as a function of ξ in the second column of table 2. The lifetime of a turbulent eddy is related to some appropriately weighted mean turnover time τ_0. A reasonable estimate is $\tau_0 \sim 2\pi$; by this time the bulk of the fluid has turned over while the central region has completed an entire rotation.

TABLE 2. TURNOVER TIMES FOR EDDIES

$\xi(\times 2/\pi)$	$t(\xi)/t(0)$	$t(\xi, 0)/t(0, 0)$	$t(\xi, \tfrac{1}{3}\pi)/t(0, 0)$	$t(\xi, \tfrac{2}{3}\pi)/t(0, 0)$
0	1·00	1·00	2·00	2·61
0·5	1·18	1·27	1·98	2·26
0·75	1·53	1·81	2·44	2·68
0·90	2·07	2·61	3·23	3·47
0·99	3·53	4·68	5·30	5·54
0·999	4·99	6·75	7·37	7·61

In three dimensions, the simplest incompressible eddy corresponds to a square convection cell with velocity

$$\mathbf{u} = (\cos x \cos y\,\mathbf{i}_x - \sin x \sin y\,\mathbf{i}_y)\sin 2z - \sin x \cos y \cos 2z\,\mathbf{i}_z, \tag{26}$$

where $\mathbf{i}_x, \mathbf{i}_y$ and $\mathbf{i}_z$ are unit vectors in the x, y and z directions. The motion lies on the vertical surfaces defined by

$$\sin y \sec x = \sin \eta = l \quad (1 \geqslant l^2 \geqslant \sin^2 y)$$

and on each surface the streamlines are given by the family of curves

$$\cos^2 x \cos 2z = \cos^2 \xi = k^2 \quad (1 \geqslant \cos^2 x \geqslant k^2).$$

The quarter period is

$$t(\xi, \eta) = \int_0^\xi \frac{\mathrm{d}x}{u_x} = \int_0^\xi \frac{\cos x \,\mathrm{d}x}{[(1 - l^2 \cos^2 x)(\cos^4 x - k^4)]^{\frac{1}{2}}}.$$

The substitution

$$\tan^2 w = \frac{1 + k^2}{2k^2}\left[\frac{1 - k^2}{\sin^2 x} - 1\right]$$

reduces this to

$$t = \frac{1}{k_1}\int_0^{\frac{1}{2}\pi} \frac{\mathrm{d}w}{(1 - k_2^2 \sin^2 w)^{\frac{1}{2}}},$$

where $\quad k_1^2 = (1 + k^2)(1 - k^2 l^2) \quad$ and $\quad k_2^2 = (1 - k^2)(1 + k^2 l^2)/k_1^2$.

The minimum value of t is

$$t(0, 0) = \pi/(2\sqrt{2}).$$

Table 2 shows $t(\xi, \eta)/t(0, 0)$ as a function of ξ for $\eta = 0, \frac{1}{3}\pi, \frac{3}{8}\pi$. The differences between the values are not great. Once again, let $\delta = \frac{1}{2}\pi - \xi \ll \frac{1}{2}\pi$; then

$$t \doteqdot \tfrac{1}{2}\ln[8/(1 - l^2)\,\delta^2] \quad \text{and} \quad \delta \doteqdot [8/(1 - l^2)]^{\frac{1}{2}}\,\mathrm{e}^{-t}.$$

When $\xi = \eta = \frac{3}{8}\pi$, the turnover time $\tau \doteqdot 6 \cdot 0$. This serves as a rough estimate of the turnover time τ_0 for the eddy as a whole and therefore of its lifetime.

(b) *Concentration of flux*

In the two-dimensional eddy defined by (25), the initial flux through the range $0 \leqslant x \leqslant \frac{1}{2}\pi$ is concentrated into the range $\xi \leqslant x \leqslant \frac{1}{2}\pi$ after a time $t(\xi)$. So the field is amplified by a factor p where

$$p(t) = \pi/2\delta \doteqdot \tfrac{1}{8}\pi\,\mathrm{e}^t \quad \text{if} \quad \delta \ll \tfrac{1}{2}\pi.$$

With the estimated lifetime of the eddy substituted we have

$$p(\tau_0) \sim 200.$$

The flow defined by (26) concentrates the field in two dimensions. Thus the amplification factor ought to be the square of that derived above. It is possible to make a rather better estimate: when $\delta \ll \frac{1}{2}\pi$, the streamlines with $l \leqslant l_0 = \sin \eta_0 < 1$ concentrate the flux into a region of area

$$A(t) = \int_0^{y_0} (x - y/l_0)\,\mathrm{d}y \doteqdot 4\,\mathrm{e}^{-2t}\ln \tan\left(\tfrac{1}{4}\pi + \tfrac{1}{2}\eta_0\right).$$

So the field is amplified by a factor p and

$$p > \frac{\pi\eta_0}{16 \ln \tan\left(\frac{1}{4}\pi + \frac{1}{2}\eta_0\right)}\,\mathrm{e}^{2t}.$$

With $\eta_0 = \frac{1}{3}\pi$ and $t = \tau_0$, this yields an amplification

$$p(\tau_0) \sim 2 \times 10^4.$$

Thus a maximum concentration of order 10^3 to 10^4 may be a reasonable estimate even in the sun.

REFERENCES

Blevin, H. & Thonemann, P. C. 1962 *Nuc. Fus.* Suppl. Part 1, 55.

Bray, R. J. & Loughhead, R. E. 1964 *Sunspots.* London: Chapman and Hall.

Bullard, E. C. 1949 *Proc. Roy. Soc.* A, **199**, 413.

Clark, A., Jr. 1965 *Phys. Fluids*, **7**, 1455.

Cowling, T. G. & Hare, A. 1957 *Quart. J. Mech. Appl. Math.* **10**, 385.

Danielson, R. E. 1961 *Astrophys. J.* **134**, 289.

Danielson, R. E. 1964 *Astrophys. J.* **139**, 45.

Herzenberg, A. & Lowes, F. J. 1957 *Phil. Trans.* A, **249**, 507.

Kolb, A. C., Thonemann, P. C. & Hintz, E. 1965 *Phys. Fluids*, **8**, 1005.

Leighton, R. B. 1959 *Astrophys. J.* **130**, 336.

Leighton, R. B. 1963 *Annual review of astronomy and astrophysics*, Vol. 1 (ed. L. Goldberg). New York: Academic Press.

Leighton, R. B., Noyes, R. W. & Simon, G. W. 1961 *Astrophys. J.* **133**, 184.

Moffatt, H. K. 1965 *J. Fluid Mech.* **22**, 521.

Parker, E. N. 1963a *Astrophys. J.* **138**, 226.

Parker, E. N. 1963b *Astrophys. J.* **138**, 552.

Parker, R. L. 1966 *Proc. Roy. Soc.* A, **291**, 60.

Roberts, K. V. & Weiss, N. O. 1966 *Math. Comp.* **20**, 272.

Simon, G. W. & Leighton, R. B. 1964 *Astrophys. J.* **140**, 1120.

Sweet, P. A. 1949 *Mon. Not. R. Astr. Soc.* **109**, 507.

Sweet, P. A. 1950 *Mon. Not. R. Astr. Soc.* **110**, 69.

Thomson, J. J. 1893 *Recent researches in electricity and magnetism.* Oxford: Clarendon Press.

Thonemann, P. C. & Kolb, A. C. 1964 *Phys. Fluids*, **7**, 1455.

Ware, A. A., Forsen, H. K. & Schupp, A. A. 1962 *Phys. Rev.* **125**, 417.

Weiss, N. O. 1964a *Phil. Trans.* A, **256**, 99.

Weiss, N. O. 1964b *Mon. Not. R. Astr. Soc.* **128**, 225.